AIAA AVIATION Forum
5-9 June 2017, Denver, Colorado
23rd AIAA Computational Fluid Dynamics Conference

Improvement of Reynolds-stress and triple-product Lag models

Michael E. Olsen *
NASA Ames Research Center
Moffett Field, CA 94035

Randolph P. Lillard †
NASA Johnson Space Center
Houston, TX 77058

The Reynolds-stress and triple product Lag models were created with a normal stress distribution which was defined by the accepted 4:3:2 distribution of streamwise, spanwise and wall normal stresses, and a ratio of $\tau_w = 0.3k$ in the log layer region of high Reynolds number flat plate flow, which implies $R_{11}^+ = \frac{4}{(9/2)*.3} \approx 2.96$. More recent measurements show a more complex picture of the log layer region at high Reynolds numbers. The first cut at improving these models along with the direction for future refinements is described. Comparison with recent high Reynolds number data shows areas where further work is needed, but also shows inclusion of the modeled turbulent transport terms improve the prediction where they influence the solution. Additional work is needed to develop a model that better matches experiments, but there is significant improvement in many of the details of the log layer behavior.

Nomenclature

M_∞	free stream Mach number
R_{ij}	Reynolds-stress tensor $\left[= \overline{u_i' u_j'}\right]$
S_{ij}	strain rate tensor $\left[= \frac{1}{2}\left(\frac{\partial u_i}{\partial x_j} + \frac{\partial u_j}{\partial x_i}\right)\right]$
T_{ijk}	Turbulent transport tensor $\left[= \overline{u_i' u_j' u_k'}\right]$
Ω_{ij}	rotation rate tensor $\left[= \frac{1}{2}\left(\frac{\partial u_i}{\partial x_j} - \frac{\partial u_j}{\partial x_i}\right)\right]$
μ	molecular viscosity
μ_T	eddy-viscosity
ν	kinematic viscosity $\left[= \frac{\mu}{\rho}\right]$
ω	specific dissipation rate $\left[= \frac{\varepsilon}{\beta^* k}\right]$
$\overline{u_i'}$	Favre average Cartesian velocity fluctuation components
ρ	mass density
τ_w	wall shear
k	turbulent kinetic energy per unit mass $\left[= \frac{1}{2}\overline{u_i' u_i'}\right]$
ε	homogeneous turbulence dissipation per unit mass $[= \beta^* k\omega]$
p	static pressure
u_∞	free stream velocity
u_i	instantaneous Cartesian velocity components
x_i	Cartesian position coordinates
u_i	Favre average Cartesian mean velocity components

*Research Scientist, NASA Ames Research Center, Associate Fellow AIAA
†Research Scientist, NASA Johnson Space Center, Member AIAA

I. Introduction

Accurate computational flowfield predictions are essential for both design and operation of aerospace vehicles. As computer speeds and memory size continue to increase, Computational Fluid Dynamics (CFD) can be used to predict the flowfield around not only simple shapes but also complete vehicle configurations. The advances in computer clock speed and memory capacity have allowed the modeling of turbulent flow, at lower Reynolds numbers, using Direct Numerical Simulations (DNS). Large Eddy Simulation (LES) continues to be developed for application at higher Reynolds numbers, but for complex configurations, DNS or even LES are still impractical because the grid resolution required (in both time and space) is well beyond current computational capabilities.

Reynolds-stress turbulence models were envisioned to overcome a number of shortcomings evident in simple Boussinesq eddy-viscosity models. Although Reynolds-stress models have had a long history of development,[1,2] they have had, until recently, limited success in actually overcoming these limitations in practice. Reynolds-stress models have enjoyed a resurgence in the past few years,[2–5] with one new methodology incorporating the desired flow history effects on the Reynolds-stress tensor in a formulation that is numerically robust.[6,7] This Lag methodology[6,8–12] allowed a further expansion of the flow history to include triple velocity products in a bid to obtain more accurate and complete turbulent transport predictions. This new model,[10] denoted "TTR" for Turbulent TRansport, augments the second-moment predictions of the Lag Reynolds-stress models, adding field equations for the third-order-moments. These are an attempt to fulfill the need for turbulent transport predictions in regions of separation, where their relative importance is larger than it is for attached flows.

Previous work on these models[6,10–12] was focused on fleshing out the mathematical system that would allow reliable, robust computation of complex flowfields with the full benefit of Reynolds-stress and higher moment models. The stress-strain relationship utilized in that effort was based upon a classic, but inaccurate, outdated set of relations:

$$\tau_w = 0.3k$$
$$(R_{11}{:}R_{22}{:}R_{33}) = (4{:}3{:}2)$$

There has been much work on more complex relations in the past few decades,[13–16] and a final consensus is yet to crystallize, but there is little doubt that, for instance, the streamwise Reynolds stresses (R_{11}^+) were at least double what this relationship would predict. To be clear, the Lag models are not alone in retaining this out of date turbulent paradigm,[5] but rather appear to be the first to attempt to embody the newer experimental knowledge.

For this paper, the main changes have to do with flat plate skin friction predictions (which are now believed to be 6% too high[17–19]) and law of the wall constants (from $\kappa = 0.41, A = 5$ to $\kappa = 0.385, A = 4.2$) but more importantly the R_{11}^+ for a flat plate boundary layer. The earlier dogma yields an $R_{11}^+ = 2.96$, where the more modern data[14,20–22] show $R_{11}^+ \geq 5.5$. Initial investigation of the effects of raising this ratio showed that it did affect separation predictions slightly, but had a substantial effect on reattachment predictions for the Bachalo-Johnson bump, causing an earlier reattachment more in line with experimental data. Comparison with relatively recent experimental data,[22] which was kindly provided by the first author of that report, suggests that more work is going to be required to obtain a Reynolds-stress model that will predict the actual log law behavior of the Reynolds stresses, so separation prediction comparisons with this interim version would be premature, even though they are promising.

As the triple products depend directly on the Reynolds-stress field, increasing R_{ij} levels will generally increase T_{ijk} levels, and as the triple products appear to give a more accurate prediction of the turbulent state in regions with low production such as separated zones, the triple product models are a central focus of this paper. The low Reynolds number near-wall, region, $y^+ \leq 100$, is not a concern of this effort. The Wilcox-1988 $k-\omega$ model has been tuned to give good predictions of attached wall shear layers for both favorable and adverse pressure gradients, and this is retained as the "near-wall" model. More complex models which would handle the physics extant in this region are envisioned and under development, but are not part of this paper.

The Reynolds-stress and triple product models described in this paper are not the final product, and miss a number of key features which were revealed with the more recent high Reynolds number data. However, they are closer to that data than the previous versions. This paper describes the predictions of the TTR

model in this chrysalis version. In line with the improved predictions of the TTR model on the rotating pipe flow,[12] the triple product terms do seem to improve the model predictions in the regions where they are active, in this flowfield at the laminar/turbulent interface of the flat plate flowfield.

II. Experiment Description/Computational Methodology

II.A. Experiments

Detailed experimental results of the Reynolds stress R_{11}^+ are taken from two sources. The first source is the Driver CS0 and BS0 flowfields,[23] where the inflow boundary layers 0.3m upstream of the spinning cylinder and adverse pressure gradient have been used. This flowfield is well documented, with skin friction determined by oil flow interferometry and three component LDV velocity measurements. The CS0 flowfield is an axisymmetric flowfield, but the boundary layer height to cylinder radius is small, and it is treated here as simply a source of high quality flat plate data.

The second source is from Marusic,[22] and is the tripped boundary layer data (SP40) discussed in that paper. This is another well documented flow field, in this case the floor of a wind tunnel. The skin friction (or more correctly u_τ) was determined by a fit to a composite velocity profile(one created to match the more recent and extensive flat plate data), and streamwise velocities were measured with hot wires. The Re_θ range of this dataset is extremely high compared to most experiments of the previous century, With the exception of a few experiments[14,17,18,24] which were completed at its conclusion. As high a Reynolds number as these experiments reach, it is noted that it corresponds to the Reynolds number at the first passenger window on a business jet. Measurements extend deep into the boundary layer, into the sublayer and production peak region. For TTR model development, the details for $y^+ \geq 100$ are the object of interest. The freestream turbulence level reported for this tunnel will be used with the "Wind Tunnel" boundary conditions described below. The turbulence intensity for this tunnel is reported as $u'/u_\infty \leq 0.002$, and the measurements of u'/u_τ at the boundary layer edge are consistent with this. A selection of R_{11}^+ measurements from other experiments[14,17,18] are also compared to the model predictions.

II.B. Computation

II.B.1. Grid

The flat plate grid used (Fig. 1) is 513 × 513, with initial wall normal spacing of $10^{-8}L$ and an initial axial spacing of $10^{-4}L$. The wall normal stretching ratio is less that 1.03, and the axial stretching ratio is less that 1.02. The grid vertical extent starts at the leading edge at $0.01L$, and linearly grows to $0.3L$ at the trailing edge, very similar to grids from.[10] The grid is sufficiently fine to allow simulation of this flowfield at axial locations that are less than $0.005L$, which corresponds to a Reynolds number based on run distance and freestream velocity of 500×10^3, nominally the lowest Reynolds number at which it would be possible to have turbulent flow at normal conditions.

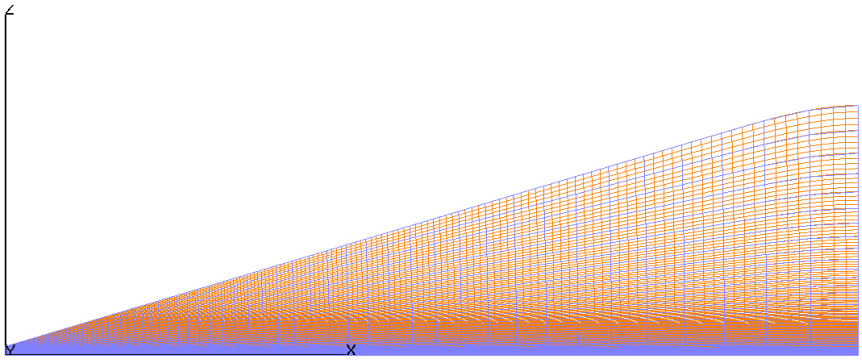

Figure 1: Flat plate grid; blue lines are every 4th grid point.

II.B.2. Boundary Value Problem Definition

The flowfield to be studied is the canonical low Mach number turbulent flat plate. This simulation is accomplished with a fully turbulent plate with a Reynolds number based on plate length of 100×10^6, which gives a long region of fully developed turbulent flow—certainly 90% of the plate length. The simulation

Mach number was set to 0.2, yielding an essentially incompressible flow field without requiring low Mach preconditioning.

The boundary conditions on the plate are viscous, adiabatic wall along $z = 0$, characteristic boundary conditions along the inflow plane and upper edge, and simple extrapolation along the exit plane. A detail that is generally not discussed at any length is the freestream conditions for k and $R_T = \frac{k}{\nu\omega}$. The standard conditions used are to set $k_\infty = 1 \times 10^{-6}$, and $Re_T = 0.1$, which is essentially laminar freestream. The turbulent kinetic energy continues to decay from the inflow edge, and k and Re_T are actually lower for any part of the solution domain without significant shear strain. This can be thought of as "Flight" conditions, where the atmospheric turbulence is vanishingly small, and this is the usual boundary condition imposed.

An alternative is to attempt to match the turbulence state existing in a wind tunnel test section, where the grid turbulence of the last screens in the settling chamber is accelerated through the contraction section, then traverses down the tunnel at a nearly constant freestream turbulence intensity. This is done by setting k to the desired level, and $Re_T \geq 1000$. If a measurement of the decay of k down the test section is available, this can be used to fix Re_T, but in this paper it is set to 1000 for the cases where non-zero freestream turbulence is being simulated. This value gives a nearly constant freestream k over the length of the plate. Choosing higher levels of Re_T give results that are essentially similar.

For most of the paper, the standard "Flight" turbulence level boundary values are used, but some results look at the effects of freestream turbulence on the model, and for those the "Wind Tunnel" method is used, with $\frac{u'}{u}|_\infty = \sqrt{\frac{2k}{3}}|_\infty$ noted.

II.B.3. Numerical Method

The code used in this study was a modified version of OVERFLOW 2.2k.[25,26] The modifications included the addition of Lag, Lag-R_{ij}, and TTR models along with the high speed modifications.[27] Matrix dissipation was used with smoothing parameters as recommended by earlier studies of high-speed flows with this code[27] with one critical change. The critical difference in the matrix dissipation smoothing parameters used is that the eigenvalue limiters are set to zero. Matrix dissipation[28] is appropriate for this flowfield.

Results from the HLLC scheme, as coded in OVERFLOW,[29,30] were compared with the matrix dissipation scheme results, and the results agree with the modified matrix dissipation scheme. The Pulliam-Chaussee diagonal scheme,[31] with variable time stepping or a constant Courant number (CFL) and multigrid was used as the relaxation method. Grid sequencing (called full multigrid in OVERFLOW) was utilized, and allowed a check on grid convergence as well as drastically reducing the CPU time required to fully converge the results

In general, spatial convective terms and diffusion terms were all second-order accurate. For the modeling of the convection terms of the turbulence models, second-order upwind was used on all the Reynolds Averaged Navier Stokes(RANS) models. The Lag methodology does require second-order accuracy (or better) since the field equations defining the lagged turbulent variables are a balance of convection and source with no diffusion terms by design—purely hyperbolic equations to accurately mimic the history effects so clearly evident in turbulent flow. In the turbulent transport level equations, not all the equations are purely hyperbolic, but they are all more driven by convection terms than standard one or two equation models.

II.B.4. Turbulence Models

For this paper, two Lag-T_{ijk} Triple product/Reynolds stress models are investigated. The baseline model is the one described in earlier papers, and includes the modifications found necessary to simulate the rotating pipe case.[12] On the flowfields described in this paper, the results obtained are essentially the same as those of the corresponding Reynolds stress model ("926").[7] The second model described here is based on that model, but with adjusted constants to obtain substantially higher R_{11}^+ values in the flat plate log layer to better match the experimental results[14,20–22,32,33] which show the much more complex behavior of the Reynolds stresses in flat plate boundary layers. Not all of this complexity is captured in this model. Regardless, the predictions are closer to experiment than the un-modified (baseline) model, and these revisions are a stepping stone to a model that captures the more complex behavior more completely.

In tuning these constants, several constraints were maintained on the turbulence model. One of the more critical, and often overlooked, is that the model give the correct decay rate for isotropic turbulence.[2] This particular constraint is important for any model that is attempting to calculate separated flowfields. In the separation region, the turbulent production becomes small, and having the decay rate correct ensures that

the dissipation, which is no longer matched by production, has the correct physical behavior. This constraint was maintained in the models described here.

The TTR model is built on top of the preceding Lag methodology models, and the equilibrium two equation turbulence model that is at their heart, the Wilcox 1988 k-ω model. The third-order-moment model comes from the exact Reynolds-stress and turbulent transport equations.

$$\begin{aligned}\partial_t\left(R_{ij}\right)+\partial_k\left(u_k R_{ij}\right) =& -R_{jk}\partial_k\overline{U_i}-R_{ik}\partial_k\overline{U_j}-\partial_k T_{ijk}+\nu\partial_k\partial_k R_{ij} \\ &+\Pi_{ij}-2\nu\overline{\partial_k(u_i')\partial_k(u_j')} \end{aligned} \tag{1}$$

$$\begin{aligned}\partial_t\left(T_{ijk}\right)+\partial_l\left(u_l T_{ijk}\right) =& -T_{ijl}\partial_l\overline{U_k}-T_{jkl}\partial_l\overline{U_i}-T_{kil}\partial_l\overline{U_j} \\ &+R_{ij}\partial_l R_{kl}+R_{jk}\partial_l R_{il}+R_{ki}\partial_l R_{jl} \\ &+\nu\partial_l\partial_l T_{ijk} \\ &+\Pi ijk-\partial_l(Q_{ijkl})-\varepsilon_{ijk}\end{aligned} \tag{2}$$

where the neglected red terms are

$$\Pi_{ij} = \frac{1}{\rho}\left[\overline{u_j'\partial_i(p')}+\overline{u_i'\partial_j(p')}\right] \tag{3}$$

$$\Pi_{ijk} = \frac{1}{\rho}\left[\overline{u_i'u_j'\partial_k(p')}+\overline{u_j'u_k'\partial_i(p')}+\overline{u_k'u_i'\partial_j(p')}\right] \tag{4}$$

$$Q_{ijkl} = \overline{u_i'u_j'u_k'u_l'} \tag{5}$$

$$\varepsilon_{ijk} = 2\nu\left(\overline{u_i'\partial_l(u_j')\partial_l(u_k')}+\overline{u_j'\partial_l(u_k')\partial_l(u_i')}+\overline{u_k'\partial_l(u_i')\partial_l(u_j')}\right) \tag{6}$$

The TTR turbulence model including turbulent transport (T_{ijk}) terms is:

$$\partial_t\left(\rho k\right)+\partial_l\left(\rho u_l k\right) = \rho\left[R_{ij}S_{ij}-\beta^* k\omega\right]+\partial_l\left(\left(\mu+\sigma_k\mu_T\right)\partial_l k\right)-A_4\partial_l\left(\rho T_{iil}\right) \tag{7}$$

$$\partial_t\left(\rho\omega\right)+\partial_l\left(\rho u_l\omega\right) = \alpha\rho S^2-\beta\rho\omega^2+\partial_l\left(\left(\mu+\sigma_\omega\mu_T\right)\partial_l\omega\right) \tag{8}$$

$$\partial_t\left(\rho R_{ij}\right)+\partial_l\left(\rho u_l R_{ij}\right) = A_0\rho\omega\left(R_{ij}^{(eq)}-R_{ij}\right) \tag{9}$$

$$\partial_t\left(\rho T_{ijk}\right)+\partial_l\left(\rho u_l T_{ijk}\right) = A_0\rho\omega\left(T_{ijk}^{(eq)}-T_{ijk}\right) \tag{10}$$

where

$$\begin{aligned}T_{ijk}^{(eq)} = & \frac{A_2}{A_0\omega}\left[T_{ijl}\partial_l\overline{U_k}+T_{jkl}\partial_l\overline{U_i}+T_{kil}\partial_l\overline{U_j}-R_{ij}\partial_l R_{kl}-R_{jk}\partial_l R_{il}-R_{ki}\partial_l R_{jl}\right] \\ &+\frac{1}{A_0\rho\omega}\left[\partial_l\left(\left(\mu+\sigma_t\mu_{t_E}\right)\partial_l T_{ijk}\right)\right]\end{aligned} \tag{11}$$

$$\begin{aligned}\mu_{t_E} &= \rho k/\omega \\ \mathcal{P} &= R_{ij}S_{ij} \\ \varepsilon &= \beta^*\rho k\omega\end{aligned} \qquad \begin{aligned}S &= \sqrt{2\left(S_{ij}S_{ij}-S_{kk}^2/3\right)} \\ S_{ij} &= \frac{1}{2}\left(\frac{\partial u_i}{\partial x_j}+\frac{\partial u_j}{\partial x_i}\right)\end{aligned}$$

Most of the parameters for this model are set by the requirement to retain the equilibrium predictions of the underlying k-ω model. The equilibrium Reynolds-stress relation is one of the three described in earlier Reynolds-stress model work,[7] denoted as the "926(Redistribution)" Equilibrium Reynolds-stress relation. This constitutive relation is most directly related to the explicit algebraic Reynolds-stress models.[34–36] The terminology is borrowed from the paper introducing this relation,[7] and contains production terms which are *not* the full Reynolds-stress production terms, but do yield log layer anisotropies consistent with the classic 4:3:2[37] relation. These "production" terms (which are actually only redistribution terms, and none of the

work terms of actual production) are

$$\mathcal{P}_{11} = 2\left(kS_{11}/A_1 + \left(R_{31}\,\Omega_{31} - R_{12}\,\Omega_{12}\right)\right) \quad (12)$$
$$\mathcal{P}_{22} = 2\left(kS_{22}/A_1 + \left(R_{12}\,\Omega_{12} - R_{23}\,\Omega_{23}\right)\right) \quad (13)$$
$$\mathcal{P}_{33} = 2\left(kS_{33}/A_1 + \left(R_{23}\,\Omega_{23} - R_{31}\,\Omega_{31}\right)\right) \quad (14)$$

with corresponding off-diagonal terms

$$\mathcal{P}_{12} = 2kS_{12}/A_1 + \left(R_{23}\Omega_{31} - R_{31}\Omega_{23} + \left(R_{11} - R_{22}\right)\Omega_{12}\right) \quad (15)$$
$$\mathcal{P}_{23} = 2kS_{23}/A_1 + \left(R_{31}\Omega_{12} - R_{12}\Omega_{31} + \left(R_{22} - R_{33}\right)\Omega_{23}\right) \quad (16)$$
$$\mathcal{P}_{31} = 2kS_{31}/A_1 + \left(R_{12}\Omega_{23} - R_{23}\Omega_{12} + \left(R_{33} - R_{11}\right)\Omega_{31}\right) \quad (17)$$

then the equilibrium Reynolds stress is given by:

$$R_{ij}{}^{(eq)} = \frac{2}{3}k\delta_{ij} - \frac{A_1}{\omega}\left(\mathcal{P}_{ij} - \frac{1}{3}\bar{\mathcal{P}}\delta_{ij}\right) + \frac{1}{A_0\rho\omega}\left[\partial_l\left(\left(\mu + \sigma_r\mu_T\right)\partial_l R_{ij}\right) - A_3\partial_l\left(\rho T_{ijl}\right)\right] \quad (18)$$

The model parameters which are constant for all TTR models in this paper are:

$$A_0 = 1.0 \qquad A_2 = 1.0 \qquad A_3 = 1.0 \qquad A_4 = 1.0$$
$$\sigma_k = 0.3 \qquad \sigma_r = 1.0 \qquad \sigma_t = 1.0$$

For the model denoted TTR(original), the remaining parameters used are:

$$A_1 = \frac{5}{3} \qquad \alpha = 0.35 \qquad \beta = 0.1 \qquad \beta^* = 0.12 \qquad \sigma_\omega = 0.3$$

while the model denoted TTR(revised) uses the parameter set

$$A_1 = \frac{10}{3} \qquad \alpha = 0.008 \qquad \beta = 0.00375 \qquad \beta^* = 0.0045 \qquad \sigma_\omega = 0.3166322$$

Note that even though β and β^* have been altered from the 1988 k-ω choices, their ratio is retained providing the same isotropic turbulence decay rate in all models.

The parameter A_1 essentially chooses R_{11}^+ in the log layer. Increasing A_1 increases the R_{11}^+ log layer value. The remaining parameters that are adjusted are chosen to maintain the isotropic decay rate discussed above, to match the log law velocity profile for a flat plate (there is a relationship between these parameters which fixes κ, much like in the analysis for the underlying k -ω(88) model[2]), and to match skin friction behavior expected for flat plate flow fields. There remains one free parameter which can be adjusted to match the flat plate skin friction relation.

The constant set (in red, which matches the color used in Fig 2) with $A_1 = \frac{5}{3}$ is labelled as "TTR" in the figures, and is essentially the original TTR model, with some minor constant adjustments that were required to work in the rotating pipe flowfield.[10] So far, these slight changes have not introduced any significant differences in other flowfields, including the one reported in this paper.

The constant set (in green, again matching the color in Fig 2) with $A_1 = \frac{10}{3}$ is labelled as "TTR(Revised)" in this paper, and while this is a stepping stone on the way, this is not expected to be the final version of the complete model. Significant improvement in details of the turbulent flowfields in wall bounded flows has been made, but there is still work yet to be done to obtain a model which matches the current experimental knowledge, which has expanded and improved greatly in the past few decades.

A full exploration focusing on separated flowfields is planned, and that paper will include a full comparison on a wide selection of flowfields, with an emphasis on separation and reattachment predictions. That work will be the model which will be used to meet the goals of the 40% improvement milestone of the Revolutionary Computational Aerosciences program.[38]

III. Results

The flat plate is the primary canonical wall-bounded turbulent flow field. Any prediction method that deals with turbulent flow over walls should be able to give reasonable predictions of this flow field to have any actual utility. For eddy viscosity models, this comes down to providing both skin friction predictions as well as matching the axial velocity profile, the law of the wall.

Recent experimental work has slightly altered both the skin friction and the κ value at the heart of the law of the wall. In previous work,[6,8–12] the Karman-Schoenherr correlation of skin friction to Re_θ was used. It was understood that there was an uncertainty in the experimental data of at least 2%,[39] but more recent work[19] has was able to obtain a much better agreement when accurate, independent measurement of the skin friction was obtained. Figure 2 shows both the original Karman-Schoenherr correlation, and Nagib's modified version of Coles-Fernholz(designated "Nagib" in that figure): $c_f'(Re_\theta) = 2\,(ln(Re_\theta)/\kappa + C)^{-2}$, with $\kappa = 0.384, C = 4.127$. The revised model can be adjusted to give skin friction reasonably close to the new correlation, at least up the highest flat plate Reynolds number data available in a ground based facility, shown by the rightmost symbol on this plot. The revised model's c_f vs. Re_θ predictions would get further and further away from the new correlation, assuming that it describes the data at higher and higher Reynolds number. For Reynolds numbers that would be involved in aircraft wing design, it is probably acceptable, but not for simulations of the entire aircraft, especially those including the fuselage. Another issue is the behavior at low Re_θ, where the model will not sustain turbulence for $Re_\theta < 1500$, a point we will return to later. For now, recall that results shown in this figure were obtained with "Flight" (vanishingly small freestream turbulence) conditions .

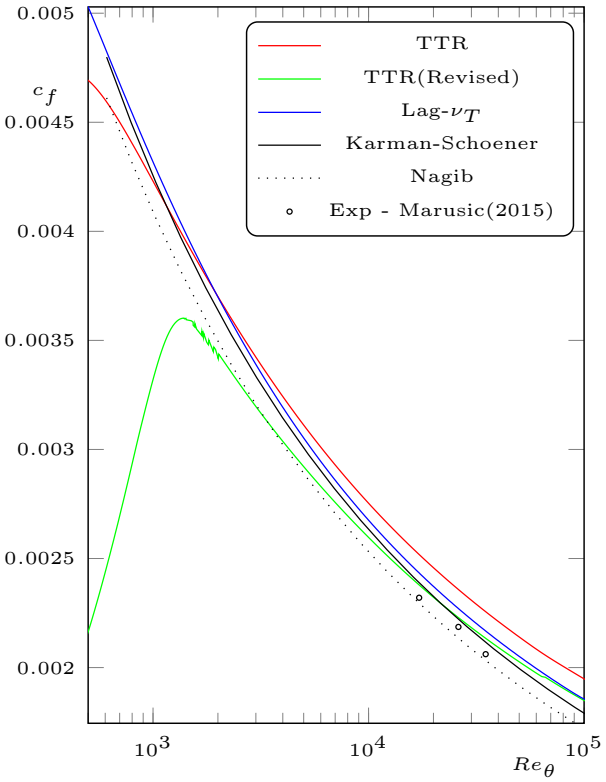

Figure 2: Flat Plate Skin Friction

The symbols plotted in Fig. 2 are derived from data obtained from,[22] and the mean velocity and R_{11}^+ profiles associated with them are shown in Fig. 3. Also included in this plot are two inflow condition profiles from the Driver CS0/BS0 flowfields. The lower portion of this plot is the velocity profile in inner coordinates (y^+, u^+). In all previous work, the Lag models have been tuned to fit the Coles log-law constants, $\kappa = 0.41$, $C = 5$. Newer data from two separate facilities with both oil flow interferometry and MEMS instruments,[17,18] along with velocity measurements give convincing evidence[40] that $\kappa = 0.385 \pm .005, C = 4.17$. The revised model fits the new log law constants. The revised model does do a better job of fitting the wake region, for both the lower and higher Reynolds number data.

The bigger difference between the baseline and revised model is shown in the top plots of Fig. 3, the normal axial Reynolds stress in inner variables, R_{11}^+ vs y^+. The baseline TTR model (and the Reynolds stress models with which it is associated) have log layer Reynolds stresses that are less than half of those of the revised version. Even with this dramatic increase of R_{11}^+ in the log layer, it is still lower than that seen experimentally in the lowest Reynolds number data that has a wide enough log layer to produce a "shelf" in R_{11}^+–red $\diamond$—data that corresponds to $Re_\theta = 17.2K$. This is the region at the start of the log layer, where $\partial_y^+ R_{11}^+ \approx 0$. For the highest Reynolds number experimental data, $Re_\theta = 35 \times 10^3$, this is $70 \leq y^+ \leq 500$.

The details for $y^+ \leq 100$ are not expected to be matched, it is the log law region $y^+ \geq 100$ that we are attempting to model. All the details below $y^+ \leq 100$ are subsumed by the underlying $k - \omega(88)$ model, which gives good skin friction predictions for favorable and adverse pressure gradients in attached boundary layers. This is a low Reynolds number region, the domain of sweep/ejection events, apparently large coherent structures, and other details that will be dealt with at later. Figure 4a focuses on the region of interest,

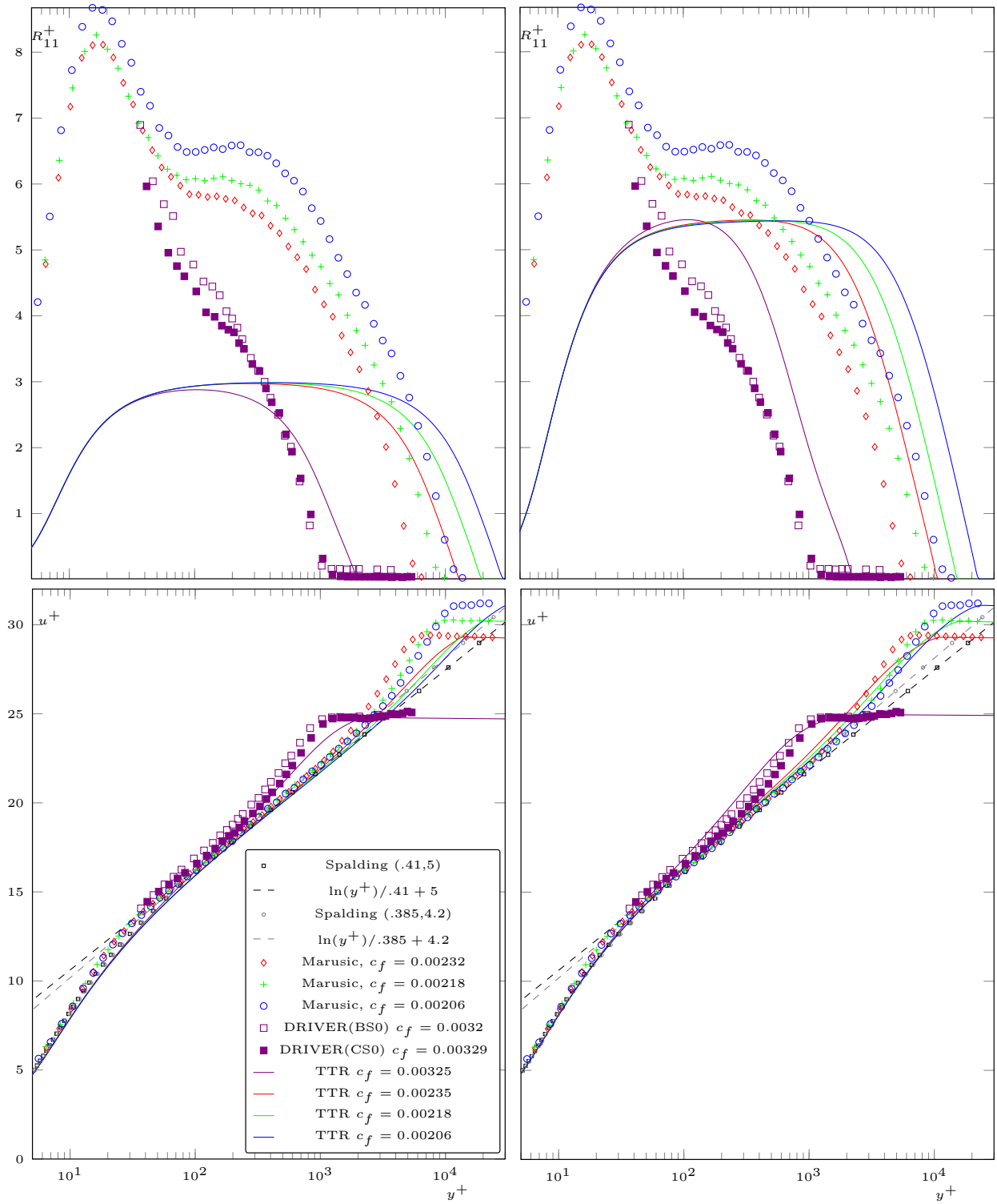

(a) TTR - Original

(b) TTR - Revised

Figure 3: Velocity(lower plot) and Axial Reynolds-stress(upper plot) in inner variables – τ_w match.

and shows some of the experimental data available from the more recent experiments. This does support the existence of a shelf, but the shelf level R_{11}^+ as a function of Re_θ is not obvious. Note that a 6% error in estimating τ_w will lead to a 6% change in R_{11}^+, and the recent changes in c_f estimates[22] are of this magnitude. Care was taken to use data that was believed to be scale resolved in this figure - indeed the data from Hites[17]

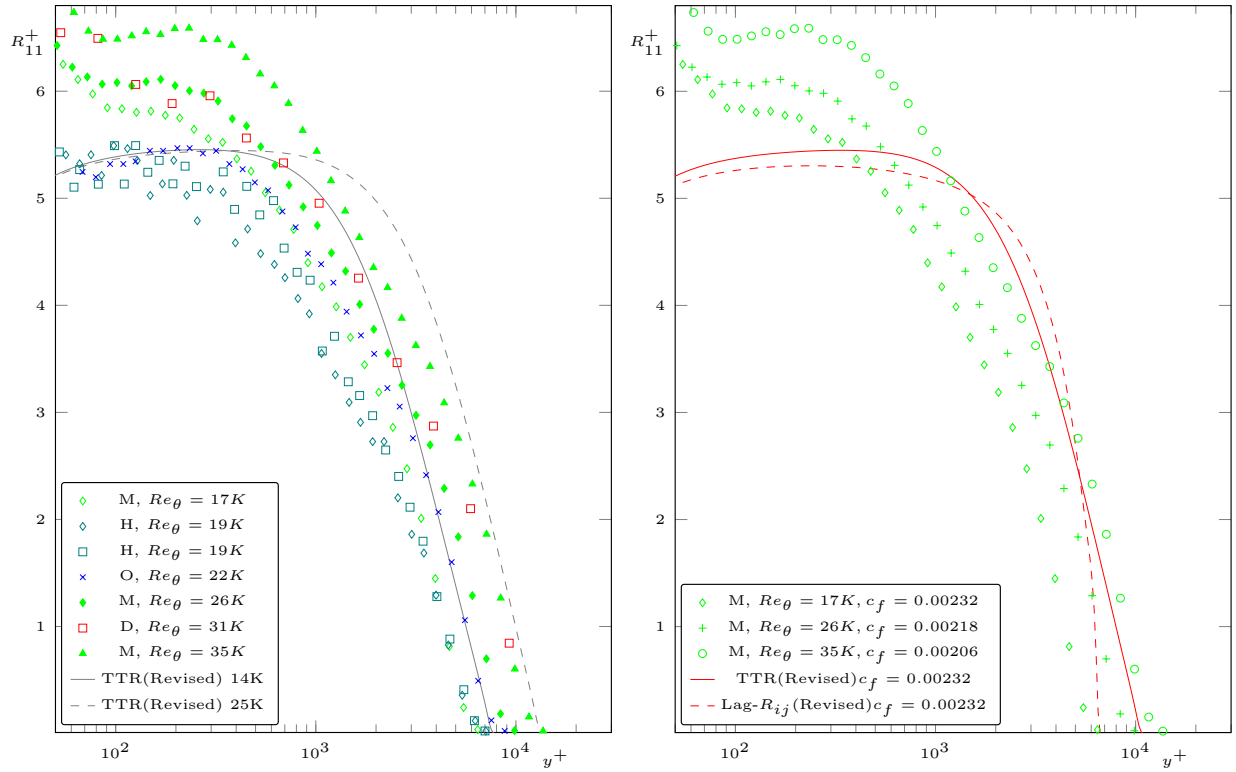

(a) R_{11}^+ Variation with Re_θ (b) Turbulent Transport Edge Prediction Improvement

Figure 4: Axial Reynolds-stress in inner variables(focus above sublayer) – Re_θ matching. Experimental data from M – Marusic,[22] H – Hites,[17] O – Österlund,[18] D –DeGraff[14]

is the data taken with two different hot wire sensors which are certainly self consistent.

The other striking miss in prediction for R_{11}^+ is that the width of the log law region, and the boundary layer itself, are too large in this revised model. Surprisingly, the revision actually is an improvement over the baseline model, as can be seen in the improved predictions at the boundary layer edge. The triple product terms in these models can seem, in some cases, to have an anti-diffusive character, and as the magnitude of these terms is proportional to the magnitude of the Reynolds-stresses, it is consistent that the higher Reynolds-stress levels of the revised model could be providing more non-diffusive assistance. One detail that bears mentioning is that it does not matter whether τ_w or Re_θ is matched between experiment and computation. Figure 3 matches τ_w, where Fig. 4a attempts a match with Re_θ. As might be expected since the model has been adjusted to match the variation of c_f with Re_θ, the conclusions about the model's R_{11} shelf extent being wider than experiment is evident in both figures.

A detail that the model is getting right is the decay from the log region plateau to the freestream floor in R_{11}^+. This can be seen in the upper right plot in Fig. 3. The plateaus are too wide, granted, but the slope of the right edge of the model prediction for $c_f = 0.00232$ red curve lines up beautifully with the right edge of the experimental data for $c_f = 0.00218$, and the experimental slopes ($\partial_{y^+} R_{11}^+$) at the three different axial locations are very similar as the freestream is approached . Note further that this is not the case for the baseline models in the upper left plot of Fig. 3, in this plot, the slope of the curves do not match as freestream is approached. This slope is directly affected by the triple product terms of the model. In the flat plate flowfield, the regions where the triple product terms have any effect are at the edges of the turbulent region, in the sublayer, and in this region at the laminar-turbulent interface at the outer edge of the boundary layer.

One of the more intriguing developments occurred as we attempted to tune the model to even higher R_{11}^+. The model was able to reproduce the log law velocity profile and follow the c_f vs. Re_θ curve, but the turbulence was not able to sustain itself until $Re_x \geq 2 \times 10^6$, a result that would be impressive in a wind tunnel used for transition research. However, up to this point, all of these simulations had been run

with free stream turbulence levels that are more like flight than wind tunnels, that is they are extremely low turbulence intensity. As a final check, this version was run with a freestream turbulence level that was consistent with a high quality (though not transition research grade) wind tunnel - a turbulence intensity level of about 0.2%. Earlier modeling work suggested that this would not significantly affect the point at which turbulence flow could be sustained by the model, but that is exactly what occurred.

With this surprising result, simulations of the TTR(Revised) model were conducted with freestream turbulence conditions that were more consistent with wind tunnel test sections, the alternative boundary condition values described above. Figure 5 shows skin friction vs. run length Reynolds number, and behavior for plausible freestream turbulence intensities is consistent with what one would expect with wind tunnels of varying freestream turbulence intensities. In this plot, the green curve ("Flight") is exactly the same simulation as is plotted in Fig. 2, except that the skin friction is plotted as a function of Re_x rather than Re_θ. Increasing the freestream turbulence level significantly lowered the run length Reynolds number Re_x at which turbulent flow could be maintained. These results were insensitive to the value of Re_T for $Re_T \geq 1000$, as these all provided a roughly constant level of k over the length of the plate. The "transition" Reynolds number thus obtained is consistent with what might be expected with the turbulence intensity changes in a wind tunnel. The TTR(Revised) model formulation is not unique in this property,[41] and in hindsight, it might have been anticipated, though these two modeling formulations are certainly distinct.

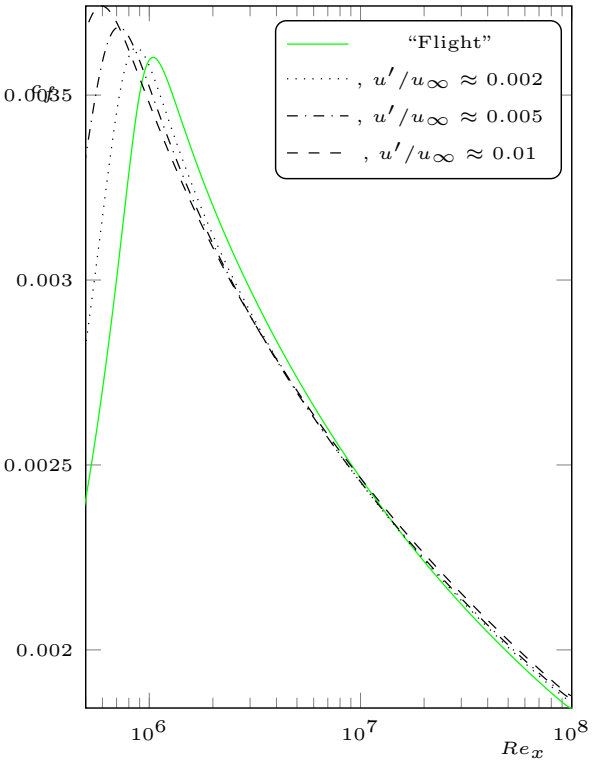

Figure 5: Effect of Freestream Turbulence level on TTR(Revised) model skin friction predictions

Having the model depend at low Reynolds number on the freestream conditions is a mixed blessing. It is not inconsistent with the model starting to pick up more and more details of the flowfield, but it adds a complexity to model development, another free parameter that needs to be assessed and understood. It may be necessary as more and more of the physical processes of the turbulent boundary layer are modelled to include this detail.

IV. Conclusions - Further Work

The modifications to the Lag-T_{ijk} (TTR) model are continuing. While the model does a better job of matching recent high Reynolds number data, there is work yet to be done in getting some of the details that are emerging. The existence of a plateau in R_{11}^+ (and presumably the other R_{ij} in the log layer) is a welcome development. If the Reynolds-stress distribution in the log layer had a more complex behavior, matching that behavior would be much more difficult.

The current model versions miss the data in two major ways. First, the model in its current form predicts a single R_{11}^+ at sufficiently high Reynolds number, and experimental data suggests that the plateau levels increase with increasing Reynolds number. Second, the plateau extent of the current formulation is overly broad, extending too high in y^+. The plateau size predicted by the model does increase with increasing Reynolds number, and with the triple product terms, it does have the correct decay in R_{11}^+ as the freestream is approached, so these details will need to be retained in the further development. A final point to be stressed is that the experimental picture (e.g. R_{11}^+ plateau levels as a function of Re_θ) is still not completely clear, and the model development is completely dependent on accurate experimental data.

The transition behavior is intriguing, but adds additional details to check, as might be expected as more physical processes are added to the turbulence model. In a flat plate flowfield, the sublayer and laminar/turbulent interface regions are the ones most affected by the addition of the triple product terms.

The TTR model revisions improve in prediction of the laminar/turbulent interface region. There are two areas in which the current model need additional improvement. The width of the plateau region of R_{11}^{+} needs to be reduced, and the R_{11}^{+} plateau level variation needs to match that of experiment. Regardless, the general improvement in prediction of the Reynolds-stress terms does seem to translate into an improvement in T_{ijk} term behaviour, based on the laminar/turbulent interface region.

A relatively famous statement was put forward by Joe Marvin[42] thirty five years ago: "No single turbulence model emerges today that applies generally to the variety of flows encountered in Computational Aerodynamics: thus turbulence modeling remains an important pacing item". Progress has been made, but this is still an accurate assessment today. The most important pacing item for turbulence modeling is detailed and complete experimental data from flowfields that can be accurately and completely modeled in CFD. The recent measurements at extremely high Reynolds number give a more detailed of the log layer, and one that suggests that there may be a field equation RANS model that can be devised to match that behavior.

Acknowledgements

The experimental data provided by Professor Ivan Marusic and used in this paper were extremely helpful, and will continue to be useful as the modeling continues.

This research was sponsored by NASA's Transformational Tools and Technologies (TTT) Project of the Transformative Aeronautics Concepts Program under the Aeronautics Research Mission Directorate.

References

[1]Pope, Stephen B., *Turbulent Flows*, Cambridge University Press, 2000.

[2]Wilcox, David C., *Turbulence Modeling for CFD*, DCW Industries, Inc, 2006.

[3]Gerolymos, G. A., Joly, S., Mallet, M., and Vallet, I., "Reynolds-Stress Model Flow Prediction in Aircraft-Engine Intake Double-S-Shaped Duct," *Journal of Aircraft*, Vol. 47, No. 4, Jul 2010, pp. 1368–1381, http://arc.aiaa.org/doi/abs/10.2514/1.47538.

[4]Cécora, R.-D., Eisfeld, B., Probst, A., Crippa, S., and Radespiel, R., "Differential Reynolds Stress Modeling for Aeronautics," AIAA Paper 2012-0465, http://dx.doi.org/10.2514/6.2012-465.

[5]Eisfeld, B. and Rumsey, C. L., *Second-Moment RANS Model Verification and Validation using the Turbulence Modeling Resource Website (Invited)*, AIAA AVIATION Forum, American Institute of Aeronautics and Astronautics, Jun 2015, 0.

[6]Lillard, R., Oliver, B., Olsen, M., Blaisdell, G., and Lyrintzis, A., "The lagRST Model: a Turbulence Model for Non-Equilibrium Flows," AIAA Paper 2012-0444, http://dx.doi.org/10.2514/6.2012-444.

[7]Olsen, M. E. , Lillard, R. P., and Murman S. M., "Separation Prediction of Large Separation with Reynolds Stress Models," AIAA Paper 2013-2720, http://dx.doi.org/10.2514/6.2013-2720.

[8]Olsen, M.E. and Coakley T. J., " The Lag Model, a Turbulence Model for Non Equilibrium Flows," AIAA Paper 2001-2564.

[9]Olsen, M., Coakley, T., and Lillard, R., *The Lag Model Applied to High Speed Flows*, American Institute of Aeronautics and Astronautics, Jan 2005, AIAA Paper 2005-101, http://dx.doi.org/10.2514/6.2005-101.

[10]Olsen, M. E., "Prediction of Separation with a Third-Order-Moment Model," AIAA Paper 2015-1968, http://dx.doi.org/10.2514/6.2015-1968.

[11]Olsen, M. E., Lillard, R. P., and Coakley, T., "LagRST Model Predictions of a Wingtip Vortex Flowfield (Invited)," AIAA Paper 2015-2923, http://dx.doi.org/10.2514/6.2015-2923.

[12]Olsen, M. E., "Reynolds-stress and triple-product models applied to flows with rotation and curvature," AIAA Paper 2016-3942, http://dx.doi.org/10.2514/6.2016-3942.

[13]Perry, A. E. and Li, J. D., "Experimental support for the attached-eddy hypothesis in zero-pressure-gradient turbulent boundary layers," *Journal of Fluid Mechanics*, Vol. 218, 1990, pp. 405438.

[14]De Graaff, David B. and Eaton, John K., "Reynolds-number scaling of the flat-plate turbulent boundary layer," *Journal of Fluid Mechanics*, Vol. 422, 11 2000, pp. 319–346, http://journals.cambridge.org/article_S0022112000001713.

[15]Knobloch, K. and Fernholz, H., *Statistics, Correlations, and Scaling in a Turbulent Boundary Layer at* $Re_{\delta_2} \leq 1.15\times10^5$, Springer Netherlands, Dordrecht, 2004, pp. 11–16.

[16]Marusic, I. and Kunkel, G. J., *Turbulence Intensity Similarity Laws For Turbulent Boundary Layers*, Springer Netherlands, Dordrecht, 2004, pp. 17–22.

[17]Hites, M. H., *Scaling of high-Reynolds number turbulent boundary layers in the National Diagnostic Facility*, Ph.D. thesis, Illinois Institute of Technology, 1997.

[18]Österlund, J. M., *Experimental Studies of Zero Pressure-Gradient Turbulent Boundary Layer Flow*, Ph.D. thesis, Royal Institute of Technolgy, Stockholm, Sweden, 1999.

[19]Nagib, H. M., Chauhan, K. A., and Monkewitz, P. A., "Approach to an asymptotic state for zero pressure gradient turbulent boundary layers," *Philosophical Transactions of the Royal Society of London A: Mathematical, Physical and Engineering Sciences*, Vol. 365, No. 1852, 2007, pp. 755–770.

[20]Smits, A. J., McKeon, B. J., and Marusic, I., "High-Reynolds Number Wall Turbulence," *Annual Review of Fluid Mechanics*, Vol. 43, No. 1, 2011, pp. 353–375, http://dx.doi.org/10.1146/annurev-fluid-122109-160753.

[21]Vallikivi, M., Hultmark, M., and Smits, A. J., "Turbulent boundary layer statistics at very high Reynolds number," *Journal of Fluid Mechanics*, Vol. 779, 9 2015, pp. 371–389, http://journals.cambridge.org/article_S0022112015002736.

[22]Marusic, I., Chauhan, K., Kulandaivelu, V., and Hutchins, N., "Evolution of zero-pressure-gradient boundary layers from different tripping conditions," *Journal of Fluid Mechanics*, Vol. 783, 2015, pp. 379–411.

[23]Driver, David M. and Johnston, James P., "Experimental Study of a Three-Dimensional Shear-Driven Turbulent Boundary Layer with Streamwise Adverse Pressure Gradient," Tech. rep., May 1990, NASA TM 102211.

[24]Saddoughi, S. G. and Veeravalli, S. V., "Local isotropy in turbulent boundary layers at high Reynolds number," *Journal of Fluid Mechanics*, Vol. 268, 06 1994, pp. 333–372, https://www.cambridge.org/core/article/local-isotropy-in-turbulent-boundary-layers-at-high-reynolds-number/1D77E82B20BF159F676C7871C1379578.

[25]Buning, P., Jespersen, D., Pulliam, T., Klopfer, G., Chan, W., Slotnick, J., Krist, S., and Renze, K., *OVERFLOW User's Manual, Version 1.8s*, NASA Langley Research Center, 2000.

[26]Jespersen, D., Pulliam, T., and Buning, P., *Recent enhancements to OVERFLOW*, American Institute of Aeronautics and Astronautics, Jan 1997, AIAA Paper 1997-0664, http://dx.doi.org/10.2514/6.1997-644.

[27]Olsen, M. and Prabhu, D., *Application of OVERFLOW to hypersonic perfect gas flowfields*, American Institute of Aeronautics and Astronautics, Jun 2001, AIAA Paper 2001-2664, http://dx.doi.org/10.2514/6.2001-2664.

[28]Swanson, R. C. and Turkel, E., "On Central–Difference and Upwind Schemes," *Journal of Computational Physics*, Vol. 101, No. 2, 1992, pp. 292–306, http://www.sciencedirect.com/science/article/pii/002199919290007L.

[29]Nichols, R. H., Tramel, R. W., and Buning, P. G., "Evaluation of Two High-Order Weighted Essentially Nonoscillatory Schemes," *AIAA Journal*, Vol. 46, No. 12, Dec 2008, pp. 3090–3102, http://arc.aiaa.org/doi/abs/10.2514/1.36849.

[30]Pulliam, T., *High Order Accurate Finite-Difference Methods: as seen in OVERFLOW*, American Institute of Aeronautics and Astronautics, Jun 2011, AIAA Paper 2011-3851, http://dx.doi.org/10.2514/6.2011-3851.

[31]Pulliam, T. and Chaussee, D., "A diagonal form of an implicit approximate-factorization algorithm," *Journal of Computational Physics*, Vol. 39, No. 2, 1981, pp. 347 – 363, http://www.sciencedirect.com/science/article/pii/002199918190156X.

[32]Hultmark, M., Vallikivi, M., Bailey, S. C. C., and Smits, A. J., "Logarithmic scaling of turbulence in smooth- and rough-wall pipe flow," *Journal of Fluid Mechanics*, Vol. 728, 8 2013, pp. 376–395, http://journals.cambridge.org/article_S0022112013002553.

[33]Dussauge, J.P., Smith, R.W., Smits, A.J., Fernhoz, H., Finley, P.J., and Spina, Eric F., "Turbulent Boundary Layers in Subsonic and Supersonic Flow," AGARDOGRAPH 335.

[34]Pope, S., "A more general effective-viscosity hypothesis," *Journal of Fluid Mechanics*, Vol. 72 (part 2), 11 1975, pp. 331–340, http://journals.cambridge.org/article_S0022112075003382.

[35]Wallin, Stefan and Johansson, Arne V., "An explicit algebraic Reynolds stress model for incompressible and compressible turbulent flows," *Journal of Fluid Mechanics*, Vol. 403, 1 2000, pp. 89–132, http://journals.cambridge.org/article_S0022112099007004.

[36]Hellsten, Antti, *New two equation Turbulence Model for Aerodynamic Applications*, Ph.D. thesis, Helsinki University of Technology, February 2004.

[37]Townsend, A. A., *The structure of turbulent shear flow*, Cambridge University Press, 2nd ed., 1976.

[38]Bonis, J., Rumsey, C., and Malik, M., "Test Cases for NASA's Revolutionary Computational Aerosciences Technical Challenge," January 2015, [Online; accessed 10-April-2017], https://turbmodels.larc.nasa.gov/StandardTestCasesFinal6.pdf.

[39]Bardina, J. E., Huang, P. G., and Coakley, T., "Turbulence Modeling Validation, Testing, and Development," Tech. rep., April 1997, NASA TM 110446.

[40]Marusic, I., Monty, J. P., Hultmark, M., and Smits, A. J., "On the logarithmic region in wall turbulence," *Journal of Fluid Mechanics*, Vol. 716, 2013.

[41]Gerolymos, G. A. and Vallet, I., chap. Bypass Transition and Tripping in Reynolds-stress Model Computations, Fluid Dynamics and Co-located Conferences, American Institute of Aeronautics and Astronautics, Jun 2013, 0.

[42]Marvin, J.G., "Turbulence Modeling for Computational Aerodynamics," *AIAA Journal*, Vol. 21, 1983, pp. 941–955.